Energy-Resolved Collision-Induced Dissociation of $Fe_2(CO)_y^+$ (y) 1 - 9)

Eugene M. Markin† and Ko-ichi Sugawara*

National Institute for AdVanced Interdisciplinary Research, National Institute of Materials and Chemical Research, Higashi 1-1-4, Tsukuba 305-8562, Japan

ReceiVed: September 24, 1999; In Final Form: December 14, 1999

Fourier transform ion cyclotron resonance mass spectrometry has been applied to the study of the energy-resolved collision-induced dissociation of di-iron carbonyl cluster cations, $Fe_2(CO)_y^+$ (y) 1 - 9). The electron impact ionization of $Fe(CO)_5$ and subsequent clustering reactions were used for the precursor ion synthesis. The sequential loss of CO ligands was observed as a typical fragmentation pathway for all $Fe_2(CO)_y^+$ clusters. Threshold values for the first ligand loss from $Fe_2(CO)_{1-9}^+$ and for the dissociation of Fe_2^+ were determined to be 1.05 (0.09, 1.23 (0.10, 1.29 (0.09, 1.25 (0.09, 0.81 (0.08, 1.10 (0.08, 0.82 (0.11, 0.33 (0.08, 1.08 (0.11, and 2.66 (0.13 eV. The sum of these 10 values is in good agreement with the literature endothermicity for the $Fe_2(CO)_9^+$ f Fe^+ + Fe + 9CO reaction. Nonmonotonic variations in the sequential thresholds are discussed in terms of spin conservation.

Introduction

An understanding of the chemical and physical properties of transition metal ions and metal - ligand ion complexes is fundamental in gas-phase ion chemistry.[1] Extensive studies over the past decade have addressed systems involving the transition-metal carbonyl cations, $M(CO)_x^+$.[1,2] An important factor in characterizing these species is the bond dissociation energy of individual metal - ligand bonds. A very versatile approach has been developed to determine the sequential bond dissociation energies by means of energy-resolved collision-induced dissociation (CID).[2] Indirectly, examination of this sequential thermochemistry provides important clues to information about the electronic states of individual $M(CO)_x^+$ ions.[3] For bare transition metal ions, the ground states have high-spin configurations, according to the number of electrons on their degenerated d orbitals. As ligands are added to the metal, this degeneracy is broken and the splitting between the orbitals increases. Finally, the ground state of the metal - ligand complex changes to a lower spin state. This spin change was experimentally observed as anomalous orderings in sequential bond dissociation energies.[3]

Much less attention has been paid to the transition metal carbonyl clusters, $M_x(CO)_y^+$, more complex systems where more than one metal center is available for coordination. Quantitative information regarding their thermochemistry is difficult to experimentally obtain due to the reactive and transient nature of these species. Synthetic methods for preparing the $M_x(CO)_y^+$ clusters in the gas phase were developed using the technique of Fourier transform ion cyclotron resonance mass spectrometry (FT-ICR). Typically, $M(CO)_y^+$ fragments formed by dissociative ionization of stable organometallic compounds readily react with their respective neutrals to give $M_x(CO)_y^+$ ionic clusters ($Fe_x(CO)_y^+$, $Cr_x(CO)_y^+$, $Ni_x(CO)_y^+$, and heteronuclear ions[4]).

This study was undertaken to establish the sequential thermochemistry of the di-iron carbonyl cluster cations, $Fe_2(CO)_y^+$ (y) 1 - 9). The ground state of Fe_2, calculated to be $^7\Delta_u$,[5] possesses the highest multiplicity among the first-row transition metal dimers,[6] while $Fe_2(CO)_9$ has a singlet ground state.[7] One can expect, therefore, that sequential ligand loss from the most ligated $Fe_2(CO)_9^+$ can be accompanied by spin changes which eventually leads to formation of Fe_2^+ with a high-spin ground state. If so, nonmonotonic variation in the sequential bond dissociation energies can be predicted for metal - ligand bonds in $Fe_2(CO)_y^+$ clusters. The averaged bond dissociation energies for $Fe_2(CO)_y^+$ (y) 1 - 4) were measured in a photodissociation study,[8] where these species were produced by the dissociative ionization of $Fe_3(CO)_{12}$. To our knowledge, however, systematic and direct studies on the sequential ligand loss and bond dissociation energies of $Fe_2(CO)_y^+$ have not yet been performed.

To obtain the dissociation thresholds for $Fe_2(CO)_y^+$, we used FT-ICR mass spectrometry in combination with energy-resolved CID measurements. In addition to the unlimited synthetic capabilities of the FT-ICR technique, much progress has been achieved during the past decade in describing the ion motion and power absorption from the rf electric field in ICR cells.[9-11] As a result, the determination of accurate ion thermochemistry in FT-ICR experiments has become available.[12-14]

Experimental Section

Precursor Ion Synthesis and Energy-Resolved CID. All experiments were performed using a Finnigan FTMS-2001 FT-ICR dual cell spectrometer equipped with a 3 T superconducting magnet. Two cubic 2 in. cells (source and analyzer cells) are collinearly aligned along the central axis of the magnetic field. The cells share a common trap plate that also serves as a conductance limit for the differential pumping. Trapping voltages were maintained at +2 V. The source cell was filled with $Fe(CO)_5$ at (4.9 - 6.6) 10^{-8} Torr. Helium was used as the collision gas for all the CID experiments and was admitted to the analyzer cell. An ionization filament was placed at a distance of 60 cm from the cell. Iron pentacarbonyl was ionized by a 3 - 5.5 ms electron pulse of nominal 20 - 70 eV energy. Ionic $Fe(CO)_y^+$ (y) 0 - 5) fragments were allowed to react with $Fe(CO)_5$ neutrals during the variable reaction delay. Appearance

* Corresponding author. E-mail: sugawara@nair.go.jp.
† Present address: Department of Chemistry, University of Waterloo, Canada.

10.1021/jp993434t CCC: $19.00 © 2000 American Chemical Society
Published on Web 02/02/2000

of $Fe_2(CO)_y^+$ (y) 3 - 8) ions as well as tri- and tetra-iron carbonyl ions in the mass spectra after the reaction delay follows the clustering sequence reported by Fredeen and Russell.[4] The ions generated in this manner were then transferred to the analyzer cell using a 150 - 180 μs grounding pulse applied to the conductance limit plate. Finally, the precursor ions were isolated in the analyzer cell by the set of standard SWIFT [15] ejection pulses with subsequent delay for collisional cooling. Complete ejection was performed for the mass ranges of the expected CID products. Typically, 2 - 4 eject-delay events were involved in the experimental sequence with a total 2.0 - 4.5 s duration of cooling delay at a He pressure of P_{He}) (0.5 - 1.7) 10^{-7} Torr. This delay time is considered to be long enough to attain thermal equilibrium between the trapped ions and the cell wall through infrared radiation and absorption. The infrared radiation lifetimes of the excited vibrational states of the ions are estimated as $10 - 10^2$ ms, since the metal - CO stretching and CO bending modes of metal carbonyls have relatively large transition dipole moments.

The $Fe_2(CO)_4^+$ and $Fe_2(CO)_5^+$ ions were the most abundant products in the above synthesis procedure. These two species served as precursors for the $Fe_2(CO)_y^+$ (y) 1 - 3) and Fe_2^+ ions, which were produced in the analyzer cell using a sustained off-resonance irradiation CID (SORI CID) technique.[16] The precursor ions isolated in the He gas were continuously accelerated - decelerated during 300 - 500 ms by an rf field applied at a frequency 500 Hz higher than their cyclotron resonances. As a result, multiple low-energy collisions with He led to efficient ligand loss.

Doublet mass peaks with a separation of around 0.05 amu appeared at m/z 280, 308, and 336, which were assigned to $Fe_2(CO)_6^+/Fe_3(CO)_4^+$, $Fe_2(CO)_7^+/Fe_3(CO)_5^+$, and $Fe_2(CO)_8^+/Fe_3(CO)_6^+$, respectively. However, ejection of $Fe_3(CO)_{4-6}^+$ was not necessary since the intensities of these ions are only 3 - 5% of those of $Fe_2(CO)_{6-8}^+$ at a reaction delay of 0.5 - 0.8 s.

The $Fe_2(CO)_9^+$ ions could not be produced by the above ion - molecule reactions. Alternatively, simple electron impact ionization of the $Fe_2(CO)_9$ molecules sublimed from solid sample was adopted.

Isolated precursor ions were translationally excited by applying a short rf pulse at the exact cyclotron frequency of the ion. The duration of the rf pulse, t_{rf}, was kept constant (90 - 160 μs). The peak-to-peak amplitude, V_{p-p}, of the excitation voltage was varied in order to change the translational energy. The ions were allowed to collide with a target gas and dissociate during the subsequent delay of t_{CID}) 2.5 - 30 ms. Dissociation products were excited before detection using a chirp excitation waveform. The product ion intensities were measured as a function of the center-of-mass collision energy, E. The average collision number of the $Fe_2(CO)_y^+$ ions is estimated to be around 0.1 under typical conditions, i.e., t_{CID}) 10 ms, P_{He}) 1 10^{-7} Torr, and E) 1 eV.

Energy Scale. The center-of-mass energy of the parent ion, corresponding to the maximum internal energy that can be converted from the translational energy upon a single collision with a stationary target gas, is given by E) $E_{lab}m_{target}/(M_{ion} + m_{target})$, where M_{ion} and m_{target} are the masses of the parent ion and target, respectively. The nominal laboratory frame energy, E_{lab}, is proportional to the squares of the ion cyclotron frequency, f, and orbital radius, r, as E_{lab}) $2\pi^2f^2r^2M_{ion}$. Assuming that the parent ion is stationary prior to the acceleration, its final cyclotron radius is given by

$$r = \beta V_{p-p} t_{rf}/2aB \quad (1)$$

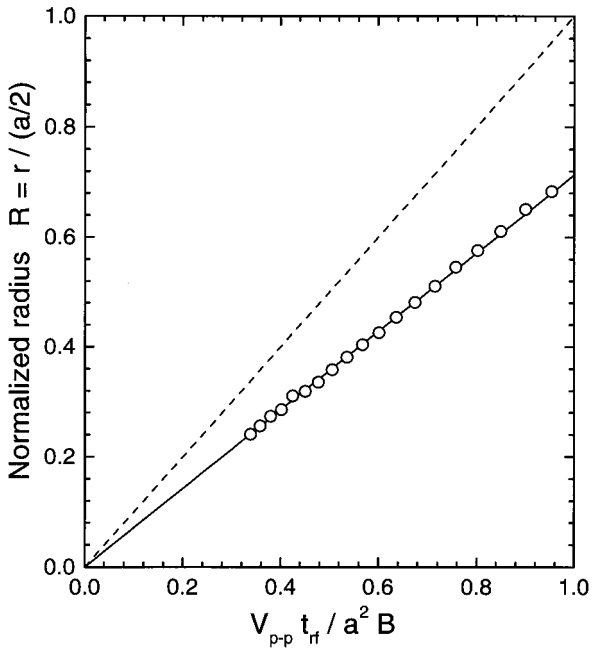

Figure 1. Normalized postexcitation ICR radius R) $r/(a/2)$ for $Fe(CO)_5^+$ as a function of $V_{p-p}t_{rf}/a^2B$. The radius R was estimated from the measurements of magnitude-mode peak heights at the third harmonic and fundamental frequency. The slope of the solid line gives a geometry factor of β) 0.714 (0.009. The dashed line represents infinite electrode approximation (β) 1).

where β) 0.72167 is the cubic cell geometry factor, a is the cell size, and B is the magnetic field strength.[11] To establish the accuracy of the ion energy scale, we applied the method of Grosshans and Marshall[10] developed for the experimental determination of an average cyclotron radius of an ion packet. The $Fe(CO)_5^+$ ions were detected after on-resonance excitation under collision-free conditions at t_{rf}) 160 μs and V_{p-p}) 17.0 - 47.8 V. Figure 1 shows the normalized postexcitation radius R) $r/(a/2)$ as a function of the normalized radius, $V_{p-p}t_{rf}/a^2B$, calculated from instrumental parameters V_{p-p} and t_{rf} for the infinite excitation electrode approximation (β) 1). The former radius R is determined from the relationship, $I(3\omega)/I(\omega)$ $0.3396R^2 + 0.01485R^3 - 0.1051R^4 + 0.04731R$,[5] where $I(3\omega)$ and $I(\omega)$ are the magnitude-mode peak heights at the third harmonic and fundamental frequencies, respectively.[10] The linear relationship shown in Figure 1 gives a geometry factor of β) 0.714 (0.009. Therefore, the postexcitation radius, r, given by eq 1, is accurate within 2% and the relative uncertainty of the collision energy scale is estimated to be 4%.

For the parent ions irradiated by the rf pulse, the spread in kinetic energy, ΔE_{lab}, arises from the original energy distribution and out-of-phase acceleration, ΔE_{lab}) $\epsilon + (E_{lab})^{1/2}\epsilon^{1/2}$, where ϵ is the original spread in the thermal energies.[17] The choice of He gas as a target partner minimizes the value of $\Delta E_{lab}/E_{lab}$, which is the most uncertain factor in the energy-resolved measurements with FT-ICR since one cannot experimentally estimate the spread. Assuming that the original energy distribution of the parent ions is the 2-D Boltzmann type at 298 K, the uncertainties in the center-of-mass collision energy due to the beam spread are calculated to be less than 0.03 - 0.05 eV at typical dissociation thresholds.

Data Analysis. The data analysis details have already been described in a previous paper.[18] The threshold curves representing the center-of-mass energy dependence of the product ion

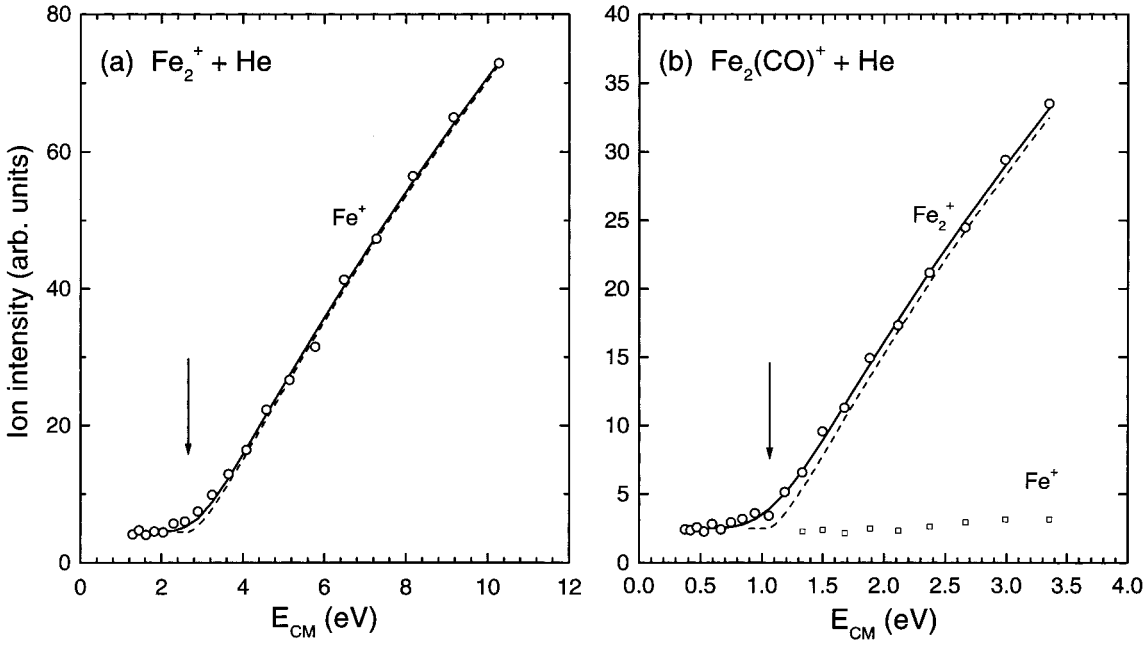

Figure 2. Threshold curves for dissociation products of (a) Fe_2^+ (t_{CID}) 7.5 ms, P_{He}) 1.5 10^{-7} Torr) and (b) $Fe_2(CO)^+$ (t_{CID}) 2.5 ms, P_{He}) 1.6 10^{-7} Torr). Solid and dashed lines indicate fitted threshold curves and model functions (eq 2). Arrows are thresholds.

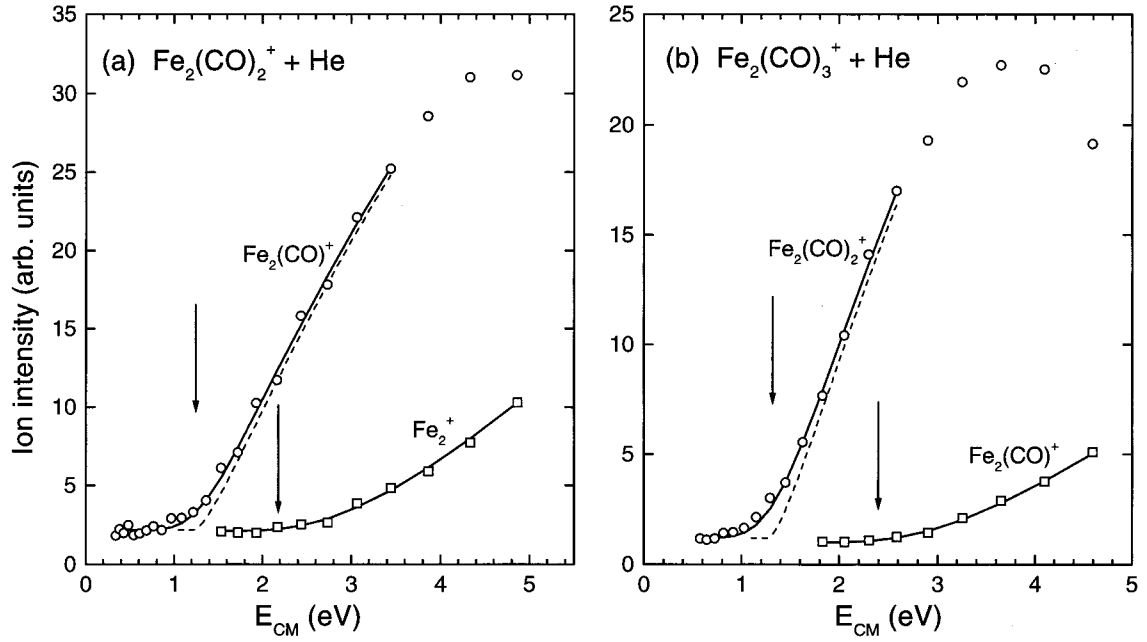

Figure 3. Threshold curves for dissociation products of (a) $Fe_2(CO)_2^+$ (t_{CID}) 2.5 ms, P_{He}) 1.5 10^{-7} Torr) and (b) $Fe_2(CO)_3^+$ (t_{CID}) 3 ms, P_{He}) 1.6 10^{-7} Torr).

intensity were analyzed with an empirical model,[19-21]

$$\sigma(E) \) A(E - E_t)^n/E \quad (2)$$

where E_t is a threshold energy, A is an energy-independent scaling factor, and n is a variable. The thermal motion of the target gas creates a Doppler-broadened distribution of relative interaction energies, E, for a given nominal center-of-mass energy, E_0. The experimentally observed cross section, $\sigma_{exp}(E_0)$, is therefore given by

$$\sigma_{exp}(E_0) \) \int_0^\infty (E/E_0)^{1/2} f(E,E_0)\, \sigma(E)\, dE \quad (3)$$

Here, $f(E,E_0)$ is the distribution function derived by Chantry[22] and the $(E/E_0)^{1/2}$ factor accounts for the difference in the interaction paths of the ions at different nominal energies. To deduce the functional form of the true cross section, the model function (eq 2) was convolved with the energy distribution, $f(E,E_0)$. The parameters A, E_t, and n were optimized using a nonlinear least-squares analysis to provide the best fit of $\sigma_{exp}(E_0)$ to the experimental data.

Results and Discussion

Threshold Curves and Dissociation Energies. Examples of the threshold curves recorded for the CID of Fe_2^+ and $Fe_2(CO)_y^+$ are shown in Figures 2-6. The sequential elimination of CO ligands from $Fe_2(CO)_y^+$ (y) 1-9) is observed:

$$Fe_2(CO)_y^+ + He \rightarrow Fe_2(CO)_{y-a}^+ + aCO + He \quad (4)$$

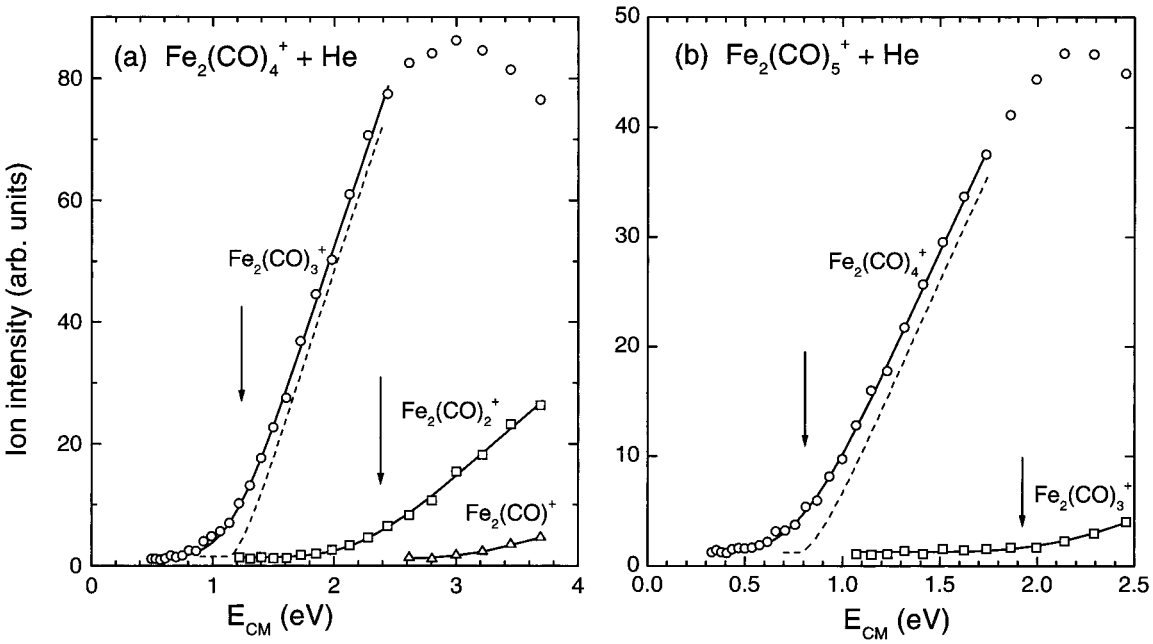

Figure 4. Threshold curves for dissociation products of (a) $Fe_2(CO)_4^+$ (t_{CID}) 10 ms, P_{He}) 1.2 10^{-7} Torr) and (b) $Fe_2(CO)_5^+$ (t_{CID}) 10 ms, P_{He}) 1.1 10^{-7} Torr).

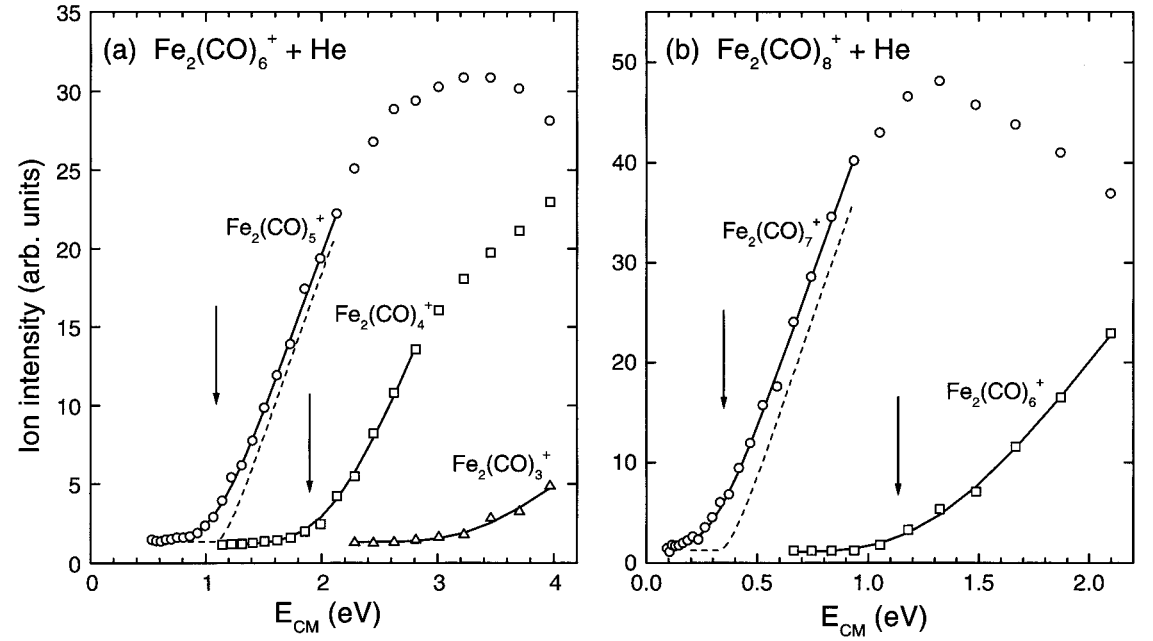

Figure 5. Threshold curves for dissociation products of (a) $Fe_2(CO)_6^+$ (t_{CID}) 12.5 ms, P_{He}) 1.0 10^{-7} Torr) and (b) $Fe_2(CO)_8^+$ (t_{CID}) 15 ms, P_{He}) 8.2 10^{-8} Torr).

The solid lines in each figure indicate the results of the best fit of $\sigma_{exp}(E_0)$ to the experimental data. The curves for the primary fragmentation products, $Fe_2(CO)_{y-1}^+$, rise almost linearly from thresholds and reach maxima with increasing collision energy. The sharp features of true cross sections, $\sigma(E)$, at the thresholds (dashed lines in Figures 2 - 6) are masked by the Doppler broadening, which is reflected in the shape of the experimental curves. Typical n values are in the range of 1.42 - 1.73. To minimize the effect of multiple collisions, the energy thresholds were determined as functions of helium pressure, P_{He}) (0.5 - 1.7) 10^{-7} Torr, and CID delay, t_{CID}) 2.5 - 30 ms. With decreasing P_{He} and t_{CID}, the threshold values increased and finally reached constant values. The thresholds obtained at the lowest P_{He} and t_{CID} in the constant region are summarized in Table 1. The listed uncertainties are the root-mean-square average of the uncertainties related to the ion energy scale, beam spread, fitting procedure, and effect of multiple collisions.

Curves for the secondary products, $Fe_2(CO)_{y-2}^+$, shown in Figures 2 - 6, have been analyzed to determine the thresholds for the loss of successive CO ligands. The difference between the secondary and primary thresholds for the CID of $Fe_2(CO)_y^+$ corresponds to the primary threshold for the CID of $Fe_2(CO)_{y-1}^+$. The secondary product intensities rise quite slowly (n) 1.58 - 2.18), and the threshold values obtained from their analysis are generally less accurate. We found that the secondary thresholds were more sensitive to the effect of multiple collisions and had larger shifts to higher energy as P_{He} and t_{CID} decreased. These observations lead to the conclusion that the data obtained from the difference between the secondary and primary thresholds can give only the lower limits of E_t. Nevertheless, these values

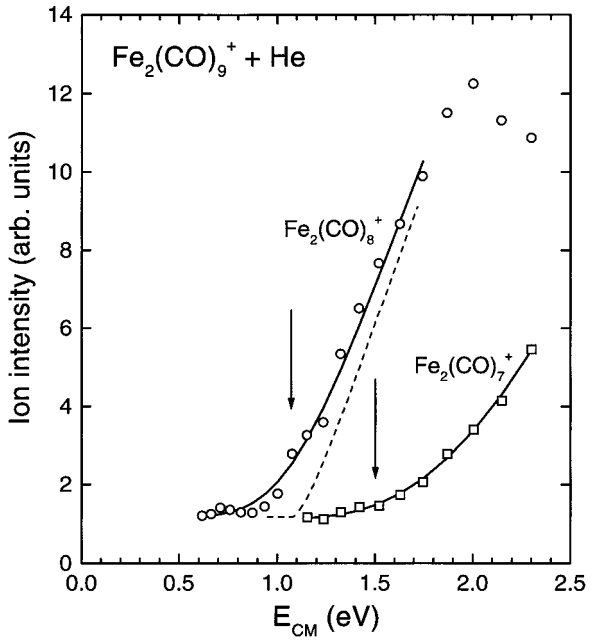

Figure 6. Threshold curves for dissociation products of $Fe_2(CO)_9^+$ (t_{CID}) 30 ms, P_{He}) 4.9 10^{-8} Torr).

TABLE 1: Summary of Measured Threshold Values E_t (eV)

process	E_t	E_t (lower limit)[a]	literature
Fe_2^+ f Fe^+	2.66 (0.13		2.43 - 2.92[b] 2.74 (0.10[c]
Fe_2CO^+ f Fe_2^+	1.05 (0.09	0.95 (0.16	< 2.54[d]
$Fe_2(CO)_2^+$ f Fe_2CO^+	1.23 (0.10	1.13 (0.07	
$Fe_2(CO)_3^+$ f $Fe_2(CO)_2^+$	1.29 (0.09	1.20 (0.14	
$Fe_2(CO)_4^+$ f $Fe_2(CO)_3^+$	1.25 (0.09	1.12 (0.15	
$Fe_2(CO)_5^+$ f $Fe_2(CO)_4^+$	0.81 (0.08	0.79 (0.13	
$Fe_2(CO)_6^+$ f $Fe_2(CO)_5^+$	1.10 (0.08	-	
$Fe_2(CO)_7^+$ f $Fe_2(CO)_6^+$	-	0.82 (0.11	
$Fe_2(CO)_8^+$ f $Fe_2(CO)_7^+$	0.33 (0.08	0.36 (0.16	
$Fe_2(CO)_9^+$ f $Fe_2(CO)_8^+$	1.08 (0.11		

[a] The lower limit of E_t for $Fe_x(CO)_y^+$ is the difference between secondary and primary thresholds measured for the CID of $Fe_x(CO)_{y+1}^+$. [b] Reference 24. [c] Reference 25. [d] Reference 8.

demonstrate good consistency with those directly measured, as indicated in Table 1. In the case of $Fe_2(CO)_7^+$, direct measurements of E_t were impossible due to the relatively weak intensity of the parent ion formed in the ion - molecule clustering reaction. The secondary threshold analysis for the CID of $Fe_2(CO)_8^+$ (Figure 5b) was the only source for the $Fe_2(CO)_7^+$ thermochemistry.

Comparison with Literature Thermochemistry. Assuming that there are no activation barriers to dissociation with excess endothermicity, the threshold values determined in the present study are taken as being equal to the individual bond dissociation energies. This assumption is well established for metal carbonyl ions,[23] where dissociation is treated as a heterolytic bond cleavage process. Comparison of the measured threshold values with literature thermochemistry data is also given in Table 1. The value E_t) 2.66 (0.13 eV for the CID of Fe_2^+ is in good agreement with those obtained in previous measurements. Brucat et al. set the limits of 2.43 e $D°(Fe_2^+)$ e 2.92 eV using the photofragmentation of jet-cooled Fe_2^+.[24] Later, Armentrout and co-workers studied the CID of Fe_n^+ (n) 2 - 19) in guided ion beam experiments and reported $D°(Fe_2^+)$) 2.74 (0.10 eV.[25]

To our knowledge, the only direct source of average metal - ligand bond energies for $Fe_2(CO)_y^+$ is the study of Russell and co-workers.[8] In their laser-ion beam experiments, a typical photodissociation process was a 2 - 3 ligand loss from $Fe_2(CO)_y^+$ (y) 1 - 5). Upper limits of the average bond dissociation energies were obtained by dividing the photodissociation threshold energy by the number of ruptured metal - ligand bonds in $Fe_2(CO)_y^+$, i.e., 2.54 eV for Fe_2CO^+ f Fe_2^+ (Table 1), 1.27 eV for $Fe_2(CO)_2^+$ f Fe_2^+, and 0.85 eV for $Fe_2(CO)_4^+$ f Fe_2CO^+.[8] In contrast, Figures 2 - 6 clearly demonstrate that the thresholds for the first and subsequent ligand loss processes are resolved in the present CID experiments. The above upper limit values estimated in the photodissociation study [8] are consistent with the corresponding values (1.05 (0.09, 1.14 (0.07, and 1.26 (0.06 eV) obtained from each threshold listed in Table 1, except the last one.

TABLE 2: Literature Thermochemistry

species	$\Delta_f H°$ (298 K) (kcal mol^{-1})
CO	- 26.42 (0.04[a]
Fe	99.31 (0.06[a]
Fe^+	283.02 (0.06[b,c]
$Fe_2(CO)_9$ (g)	- 319 (6[d]
$Fe_2(CO)_9^+$	- 135.1 (6[c,e]

[a] Reference 26. [b] IE(Fe)) 7.9024 (0.0001 eV.[27] [c] Includes 1.48 kcal mol^{-1} for the enthalpy of the electron (thermal electron convention). [d] Reference 28. [e] IE[$Fe_2(CO)_9$]) 7.91 (0.01 eV.[29]

The sum of 10 threshold values listed Table 1 must agree with the enthalpy for complete fragmentation of $Fe_2(CO)_9^+$ in reaction 5, $\Delta_r H°(5)$:

$$Fe_2(CO)_9^+ \text{ f } Fe^+ + Fe + 9CO \qquad (5)$$

The enthalpy of formation for CO,[26] Fe,[26] and Fe^+ [26,27] is well established (Table 2). Connor et al. reported the value of $\Delta_f H°[Fe_2(CO)_9(g)]$) - 319 (6 kcal mol^{-1}, based on the enthalpy of formation measured for the solid, $\Delta_f H°[Fe_2(CO)_9$-(c)]) - 337 (3 kcal mol^{-1}, and the estimated enthalpy of sublimation, ΔH_{sub}) 18 (5 kcal mol^{-1}.[28] The value of $\Delta_f H°[Fe_2(CO)_9^+]$) - 135.1 (6 kcal mol^{-1} was calculated using the ionization potential data, IE[$Fe_2(CO)_9$]) 7.91 (0.01 eV, reported by Junk et al.[29]

Finally, from the literature thermochemistry data listed in Table 2, we derived the enthalpy change in reaction 5 of $\Delta_r H°(5)$) 279.6 (6 kcal mol^{-1} (12.12 (0.26 eV) at 298 K. Summation of the 10 experimentally determined thresholds, E_t, listed in Table 1 gives the endothermicity of the complete $Fe_2(CO)_9^+$ fragmentation, 268.0 (7.2 kcal mol^{-1} (11.62 (0.31 eV), which is in good agreement with $\Delta_r H°(5)$ within the combined error. The uncertainties of 0.08 - 0.13 eV (Table 1) for the E_t values are likely the practical limit of energy-resolved CID experiments with FT-ICR. Reference measurements reported earlier for this technique also demonstrated that the dissociation thresholds deviate about 0.1 - 0.2 eV from values cited in the literature.[12 - 14]

Trend in Dissociation Energies. The dissociation energies of $Fe_2(CO)_y^+$ (y) 1 - 9) obtained in this study are plotted in Figure 7 as a function of the number of CO ligands. For comparison, we also present the sequential bond dissociation energies for $Fe(CO)_y^+$ (y) 1 - 5) reported by Armentrout and co-workers (squares combined with a dashed line in Figure 7).[30] One can see a nonmonotonic variation in the energetics of di-iron carbonyls as the degree of ligation changes, which is similar to the transition metal - carbonyl ion complexes $M(CO)_y^+$.[3] This similarity provides a chance to explain the nonmonotonic trend in terms of changes in the spin of metal carbonyls that

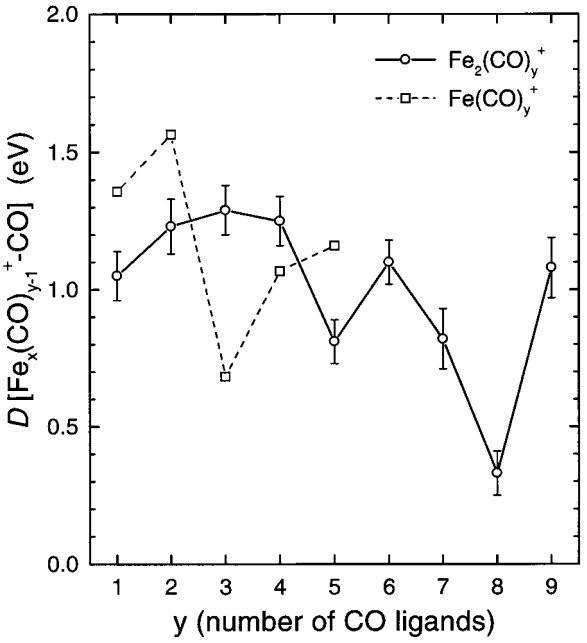

Figure 7. Bond dissociation energies for $Fe_2(CO)_y^+$ (circles and solid line) and $Fe(CO)_y^+$ (squares and dashed line),[23] as a function of the number of CO ligands, *y*.

accompany the removal of the CO ligands. Relatively high thresholds, for example, were associated with the spin-allowed dissociations in the cases of $Fe(CO)_4^+$ and $Fe(CO)_5^+$.[30] Dissociation along an adiabatic surface, from doublet $Fe(CO)_3^+$ to quartet $Fe(CO)_2^+$, was postulated to explain the much lower dissociation threshold for the CID of $Fe(CO)_3^+$.[30]

Since $Fe_2(CO)_9$ is known to have a singlet ground state,[7] the $Fe_2(CO)_9^+$ cation is likely to be a doublet. Recently, Jacobsen and Ziegler investigated the structure and energetics of several isomers of $Fe_2(CO)_8$.[31] A doubly bridged C_s structure in a singlet state was calculated to be the most stable, as predicted in a matrix-isolation IR spectroscopic study.[32] They also found an unbridged D_{3d} structure in a triplet state at 1.09 eV higher than the C_s structure. However, the IR spectrum of the unbridged $Fe_2(CO)_8$ was not consistent with the D_{3d} structure. Thus, one can assume that the $Fe_2(CO)_8^+$ cation has a doublet ground state and there is no spin change for the CID of $Fe_2(CO)_9^+$.

The ground state of Fe_2 was calculated to be $^7\Delta_u$ by Shim and Gingerich.[5] It is very likely that Fe_2CO also has a ground state with a high-spin configuration. For the Fe_2N_2 system, the ground state was calculated to be a quintet in both cases where the N_2 axis is either parallel or perpendicular to the Fe_2 bond.[33] As CO ligands are successively removed from $Fe_2(CO)_9^+$, the spin state of $Fe_2(CO)_y^+$ should change somewhere between $Fe_2(CO)_8^+$ and Fe_2^+. A remarkably low threshold for the CID of $Fe_2(CO)_8^+$ may imply that this is due to the spin change and, more speculatively, that $Fe_2(CO)_7^+$ possesses a quartet ground state. The bond dissociation energy of $Fe_2(CO)_5^+$ is also weaker than those of $Fe_2(CO)_{1-4}^+$ and $Fe_2(CO)_6^+$, as shown in Figure 7. If we further postulate that $Fe_2(CO)_6^+$ and $Fe_2(CO)_5^+$ have quartet ground states, then the low threshold for the ligand loss from $Fe_2(CO)_5^+$ may again reflect fragmentation along an adiabatic surface with a low lying higher spin asymptote (presumably a sextet) for the $Fe_2(CO)_4^+$ dissociation product. The thresholds for $Fe_2(CO)_{2-4}^+$ are relatively high and their dissociation processes are believed to be spin-allowed. It is very likely, therefore, that the ground states of $Fe_2(CO)_{1-4}^+$ are sextets. In addition to these qualitative hypotheses, one can expect a spin change from the sextet to octet for ligand loss from $Fe_2(CO)^+$. Unfortunately, these unambiguous statements cannot be clarified, since data on the electronic structure of the di-iron carbonyl cations are not available for direct comparison. It is not unusual, however, that a spin change induced by increasing the ligand field is responsible for the nonmonotonic trend in the dissociation thresholds on the way from a high-spin bare iron dimer cation to the doublet ground state of the highly ligated $Fe_2(CO)_8^+$ and $Fe_2(CO)_9^+$ ions.

Conclusions

The dissociation of di-iron carbonyl cations, $Fe_2(CO)_y^+$, has been examined by means of energy-resolved CID uisng a FT-ICR mass spectrometer. In contrast to the earlier photodissociation studies, elimination of one CO molecule was observed as the primary fragmentation pathway. We reported the first direct measurements of the energy thresholds for the CID of $Fe_2(CO)_y^+$ (y) 1 - 9). The total of these nine values together with the threshold for the Fe_2^+ dissociation gives good agreement with the literature thermochemistry data for the complete fragmentation of $Fe_2(CO)_9^+$. The nonmonotonic trend in the sequential thresholds demonstrates similarities with monatomic metal - ligand ion complexes. The relatively low stability of $Fe_2(CO)_5^+$ and $Fe_2(CO)_8^+$ suggests dissociation along an adiabatic surface with a low-lying higher spin asymptote for their CID products.

Acknowledgment. The authors are grateful to H. Takeo for the valuable discussions and his continuous support. E.M.M. is indebted to the Agency of Industrial Science and Technology (AIST) for the award of a stipend.

References and Notes

(1) Freiser, B. S. *J. Mass Spectrom.* **1996**, *31*, 703.
(2) Armentrout, P. B.; Kickel, B. L. In *Organometallic Ion Chemistry*; Freiser, B. S., Ed.; Kluwer Academic Publishers: Dordrecht, 1996; p 1.
(3) Armentrout, P. B. *Acc. Chem. Res*. **1995**, *28*, 430.
(4) Fredeen, D. A.; Russell, D. H. *J. Am. Chem. Soc*. **1985**, *107*, 3762; **1986**, *108*, 1860.
(5) Shim, V.; Gingerich, K. A. *J. Chem. Phys*. **1982**, *77*, 2490.
(6) Morse, M. D. *Chem. Re*V. **1986**, *86*, 1049.
(7) Freundlich, H.; Cuy, E. J. *Ber*. **1923**, *56*, 2264.
(8) Tecklenberg, R. E., Jr.; Bricker, D. L.; Russell, D. H. *Organometallics* **1988**, *7*, 2506.
(9) Schweikhard, L.; Marshall, A. G. *J. Am. Soc. Mass. Spectrom*. **1993**, *4*, 433.
(10) Grosshans, P. B.; Marshall, A. G. *Int. J. Mass Spectrom. Ion Processes* **1992**, *115*, 1.
(11) Grosshans, P. B.; Marshall, A. G. *Int. J. Mass Spectrom. Ion Processes* **1990**, *100*, 347.
(12) Katritzky, A. R.; Watson, C. H.; Dega-Szafran, Z.; Eyler, J. R. *J. Am. Chem. Soc*. **1990**, *112*, 2471.
(13) Hop, C. E. C. A.; McMahon, T. B.; Willett, G. D. *Int. J. Mass Spectrom. Ion Processes* **1990**, *101*, 191.
(14) Sievers, H. L.; Grützmacher, H.; Caravatti, P. *Int. J. Mass Spectrom. Ion Processes* **1996**, *157/158*, 233.
(15) Wang, T.-C. L.; Ricca, T. L.; Marshall, A. G. *Anal. Chem*. **1986**, *58*, 2935.
(16) Gauthier, J. W.; Trautman, T. R.; Jacobson, D. B. *Anal. Chim. Acta* **1991**, *246*, 211.
(17) Huntress, W. T., Jr.; Mosesman, M. M.; Elleman, D. D. *J. Chem. Phys*. **1971**, *54*, 843.
(18) Markin, E. M.; Sugawara, K. *Eur. Mass Spectrom*. **1999**, *5*, 235.
(19) Chesnavich, W. J.; Bowers, M. T. *J. Phys. Chem*. **1979**, *83*, 900.
(20) Boo, B. H.; Armentrout, P. B. *J. Am. Chem. Soc*. **1987**, *109*, 3549.
(21) Boo, B. H.; Elkind, J. L.; Armentrout, P. B. *J. Am. Chem. Soc*. **1990**, *112*, 2083.
(22) Chantry, P. J. *J. Chem. Phys*. **1971**, *55*, 2746.
(23) Armentrout, P. B.; Simons, J. *J. Am. Chem. Soc*. **1992**, *114*, 8627.
(24) Brucat, P. J.; Zheng, L.-S.; Pettiette, C. L.; Yang, S.; Smalley, R. E. *J. Chem. Phys*. **1986**, *84*, 3078.

(25) Lian, L.; Su, C.-X.; Armentrout, P. B. *J. Chem. Phys.* **1992**, *97*, 4072.
(26) Chase, M. W., Jr.; Davies, C. A.; Downey, J. R., Jr.; Frurip, D. J.; McDonald, R. A.; Syverud, A. N. *J. Phys. Chem. Ref. Data, Suppl. No. 1* **1985**, *14*, 1.
(27) Sugar, J.; Corliss, C. *J. Phys. Chem. Ref. Data, Suppl. No. 2* **1985**, *14*, 1.
(28) Connor, J. A.; Skinner, H. A.; Virmani, Y. *Faraday Symp. Chem. Soc*. **1973**, *8*, 18.
(29) Junk, G. A.; Preston, F. J.; Svec, H. J.; Thompson, D. T. *J. Chem. Soc. A* **1970**, 3171.
(30) Schultz, R. H.; Crellin, K. C.; Armentrout, P. B. *J. Am. Chem. Soc*. **1991**, *113*, 8590.
(31) Jacobsen, H.; Ziegler, T. *J. Am. Chem. Soc*. **1996**, *118*, 4631.
(32) Fletcher, S. C.; Poliakoff, M.; Turner, J. J. *Inorg. Chem.* **1986**, *25*, 3597.
(33) Bauschlicher, C. W., Jr.; Pettersson, L. G. M.; Siegbahn, P. E. M. *J. Chem. Phys.* **1987**, *87*, 2129.